0026-895X/96/061625-10$3.00/0

MOLECULAR PHARMACOLOGY, 50:1625–1634 (1996).



# Evidence for an Internal Phenylalkylamine Action on the Voltage-Gated Potassium Channel Kv1.3

HEIKO RAUER and STEPHAN GRISSMER

*Department of Applied Physiology, University of Ulm, 89075 Ulm, Germany*

Received June 24, 1996; Accepted August 31, 1996

## SUMMARY

We characterized the action of verapamil and *N*-methyl-verapamil on current through the delayed-rectifier potassium channel Kv1.3 mouse (*m*Kv1.3). The whole-cell and inside-out configuration of the patch-clamp technique was used to examine the channel properties after injection of *in vitro* transcribed cRNA into rat basophilic leukemia cells. The action of verapamil on current through *m*Kv1.3 channels could be separated into an acceleration of the rate of current decay during depolarizing pulses and a reduction of steady state peak current when applied either extracellularly or intracellularly. Both effects were greatly reduced when the membrane-impermeable *N*-methyl-verapamil was applied extracellularly, but it affected current through *m*Kv1.3 channels similar to verapamil if applied to the intracellular side of the membrane. Mutations in the outer vestibule of the *m*Kv1.3 channel did not change the ability of verapamil to accelerate the *m*Kv1.3 current decay during depolarizing pulses, whereas the reduction of the steady state peak current by verapamil applied either extracellularly and intracellularly and by *N*-methyl-verapamil applied intracellularly was decreased ~25-fold in all three cases. Substances known to interact with an extracellular site of the channel (e.g., extracellularly applied tetraethylammonium or kaliotoxin) did not compete with extracellularly applied verapamil on blocking steady state peak current, whereas intracellularly applied tetraethylammonium, which is known to interact with an intracellular site of the channel, was able to reduce the effect of extracellularly applied verapamil on blocking steady state peak current, suggesting competition for a common binding site between verapamil and intracellularly applied tetraethylammonium. The results from the competition experiments as well as from the mutations in the outer vestibule of *m*Kv1.3 are compatible with the idea that verapamil applied extracellularly moves through the membrane to reach its internal binding site on the *m*Kv1.3 channel.

The voltage-gated $K^+$ channel *m*Kv1.3 is a member of the *Shaker*-related $K^+$ channel family and plays an important role in T lymphocyte activation (1–3). The "classic" voltage-gated $K^+$ channels are thought to have six transmembrane-spanning segments (S1–S6), and the amino and carboxyl termini are located intracellularly. The S4 segment contains major parts of the voltage sensor, whereas the region between segments S5 and S6 is thought to be part of the ion conduction pathway and is therefore called the pore region (4–9). It has been shown that the previously described *n*-type $K^+$ channel is predominant in T lymphocytes (1–3) and is a homologue to Kv1.3 (10, 11). T cell activation can be inhibited by Kv1.3 channel blockers such as TEA and 4-aminopyridine (1, 2). Other very potent blockers of Kv1.3 and related voltage-gated $K^+$ channels are the peptide toxins charybdotoxin, margatoxin, and KTX (12–15). Nifedipine, diltiazem, and verapamil, originally known as potent L-type $Ca^{2+}$ channel blockers, are also able to block Kv1.3 (3, 10) and therefore inhibit the T cell activation (1, 2).

This work was supported by a grant from Pfizer (Groton, CT) and the Deutsche Forschungs Gemeinschaft (Grant 848/4-1).

To map amino acid residues in the outer vestibule of the *m*Kv1.3 channel, the peptide toxins were used to obtain insight into the topology of the pore region (16). To confirm and extend these findings, we used the $Ca^{2+}$ channel antagonist verapamil and its derivative, *N*-methyl-verapamil. Because of the smaller dimensions of these compounds compared with the peptide toxins and their well-defined structures, they seemed to be good tools with which to localize additional residues that act as drug- but not toxin-binding sites at the pore region of the channel. Recently, DeCoursey (17) showed that on the *n*-type $K^+$ channel endogenously expressed in rat alveolar epithelial cells, verapamil blocked potently only if applied from the outside in the neutral form by partitioning into the membrane. Based on these findings, we wanted to localize the binding site of verapamil on the *m*Kv1.3 channel exogenously expressed in RBL cells by using mutations in the pore region. Also, if contact amino acid residues for verapamil could be identified, it should be possible in future examinations to obtain more-detailed structural information regarding the pore region. For our initial study, we used mutations at the outer vestibule of Kv1.3 that have been

**ABBREVIATIONS:** *m*Kv1.3, mouse Kv1.3; KTX, kaliotoxin; RBL, rat basophilic leukemia; TEA, tetraethylammonium; EGTA, ethylene glycol bis(β-aminoethyl ether)-*N*,*N*,*N*′,*N*′-tetraacetic acid; HEPES, 4-(2-hydroxyethyl)-1-piperazineethanesulfonic acid; FITC, fluorescein isothiocyanate.

proved to be part of the extracellular binding site for TEA (18) as well as several scorpion toxins (16).

We investigated the actions of verapamil and *N*-methyl-verapamil (D575) on current through *m*Kv1.3 and a H404T mutant channel in the whole-cell mode and in the inside-out patch configuration with application of the drugs to the inner and outer portions of the channel. Some of the results have been reported in preliminary form (19, 20).

## Materials and Methods

**Cells.** All experiments were carried out on single RBL cells (21). Cells were obtained from the American Type Culture Collection (Rockville, MD). The cells were maintained in a culture medium of Eagle's minimal essential medium supplemented with 1 mM L-glutamine and 10% heat-inactivated fetal calf serum in a humidified, 5% $CO_2$ incubator at 37°. Cells were plated to grow nonconfluently onto glass 1 day before use in injection and electrophysiological experiments.

**Solutions.** The experiments were done at room temperature (21–25°). Cells measured in the whole-cell configuration were normally bathed in mammalian Ringer's solution containing 160 mM NaCl, 4.5 mM KCl, 2 mM $CaCl_2$, 1 mM $MgCl_2$, and 10 mM HEPES adjusted to pH 7.4 with NaOH, with an osmolarity of 290–320 mOsM. Measurements in the inside-out patch configuration were done in a bath solution containing 164.5 mM K-aspartate, 1 mM $CaCl_2$, 2 mM $MgCl_2$, 10 mM HEPES, and 10 mM EGTA adjusted to pH 7.2 with KOH, with an osmolarity of 290–320 mOsM. A simple syringe-driven perfusion system was used to exchange the bath solutions in the recording chamber.

The internal pipette solution for the whole-cell recordings contained 134 mM KF, 1 mM $CaCl_2$, 2 mM $MgCl_2$, 10 mM HEPES, and 10 mM EGTA, adjusted to pH 7.2 with KOH, with an osmolarity of 290–320 mOsM. The pipette solution for the inside-out patch measurements contained normal Ringer's solution, as described above.

**Chemicals.** Verapamil was purchased from Sigma-Aldrich Chemie (Deisenhofen, Germany) as (±)-verapamil hydrochloride. *N*-Methyl-verapamil was generously provided by Drs. Raschack and Paul of Knoll Pharmaceuticals (Ludwigshafen, Germany) as *N*-methyl-verapamil hydrochloride. TEA was purchased from Fluka Chemie (Buchs, Germany) as tetraethylammonium chloride. KTX was purchased from Latoxan (Rosans, France).

TEA and KTX were dissolved in mammalian Ringer's solution. The phenylalkylamines were dissolved in dimethylsulfoxide (Fluka) to make stock solutions from which final dilutions were made. The stock solutions were stored at 4° and protected from light. The final dimethylsulfoxide concentrations diluted in the external or internal Ringer's solutions were <0.1%.

**Electrophysiology.** Experiments were carried out using the whole-cell or the inside-out patch recording mode of the patch-clamp technique (22). Electrodes were pulled from glass capillaries (Clark Electromedical Instruments, Reading, UK) in two stages, coated with Sylgard (Dow Corning, Seneffe, Belgium), and fire-polished to resistances measured in the bath of 2.5–4 MΩ. Membrane currents were recorded with an EPC-9 patch-clamp amplifier (HEKA Elektronik, Lambrecht, Germany) interfaced to a Macintosh Quadra 840AV computer running acquisition and analysis software (Pulse and PulseFit). Capacitative and leak currents were subtracted using the P/8 procedure. Series resistance compensation (80%) was used if the current exceeded 1 nA. The holding potential in all experiments was −80 mV. For drug screening, the voltage was usually stepped from −80 to +40 mV for 200 msec every 30 sec before, during, and after application of the compounds.

**Expression.** pSP64T plasmids (23) containing the entire coding sequence of the *m*Kv1.3 wild-type gene and the sequences for the mutant channels H404T and G380H (a generous gift from Dr. K. G. Chandy, University of California, Irvine, Irvine, CA) were linearized with *Eco*RI and transcribed *in vitro* with the SP6 Cap-Scribe System (Boehringer-Mannheim Biochemica, Mannheim, Germany). The resulting cRNA was phenol/chloroform purified and could be stored at −75° for several months.

The cRNA was diluted with a fluorescent FITC-dye (0.5% FITC-Dextran in 100 mM KCl) to a final concentration of 1 μg/μl. RBL cells were injected with the cRNA/FITC solution filled in injection capillaries (Femtotips) using an Eppendorf microinjection system (Micromanipulator 5171 and Transjector 5246). In the visualized cells, specific currents could be measured 3–6 hr after injection.

## Results

To initially characterize the effect of verapamil on the voltage-gated $K^+$ channel *m*Kv1.3, we measured *m*Kv1.3 currents in the presence and absence of 20 μM verapamil. The result of such an experiment is shown in Fig. 1. It shows the control *m*Kv1.3 wild-type current in the absence of verapamil (Fig. 1A, *trace 1*). The current increased rapidly on depolarization, reached a peak within 8 msec, and then decreased again with a time constant of ~230 msec (Table 1). This current decay, the C-type inactivation, is typical for *n*-type $K^+$ channels and the homologue *m*Kv1.3 (1–3, 10, 11). Trace 2 is the first trace obtained in the presence of 20 μM verapamil, and all the following traces were also recorded in verapamil. It is obvious that the application of 20 μM verapamil has two effects: (a) an acceleration of the current decay during the depolarization and (b) a reduction in the peak current amplitude from trace to trace until the peak current amplitude has reached a new steady state value. Both effects are in agreement with earlier reports (24). The acceleration of current decay may reflect the rate at which open $K^+$ channels are blocked by verapamil (24) (for more details, see below), whereas the reduction in peak current amplitude to a new steady state value might reflect accumulation of block

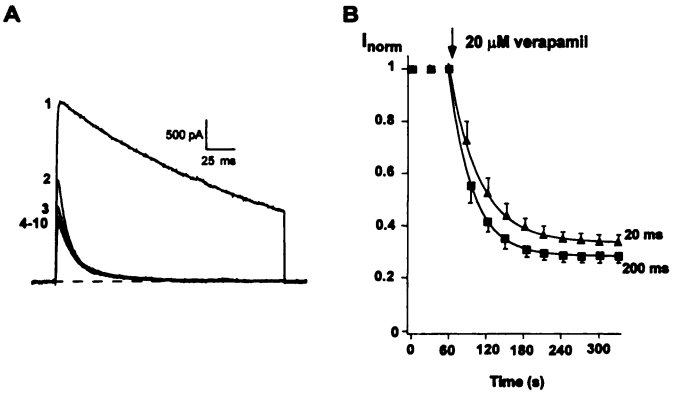


**Fig. 1.** Effect of extracellularly applied verapamil on currents through *m*Kv1.3 wild-type channels. A, Currents were elicited by 200-msec depolarizing voltage steps from a holding potential of −80 to +40 mV every 30 sec. Currents were recorded (*trace 1*) before and (*traces 2–10*) after external application of 20 μM verapamil. *Current traces 7–10*, constant current properties with a steady state peak current. B, Time course of peak current reduction by verapamil. Normalized peak currents obtained from the record shown in A and similar records were plotted against time. *Arrow*, bath solution was changed to a bath solution containing 20 μM verapamil. Time constants of peak current reduction ($\tau_{on}$) were obtained through fitting with a single-exponential function (*smooth line*) to the data. *Data points*, normalized peak current of at least three independent experiments; *bars*, mean ± standard deviation. At 200-msec voltage-step duration (■), $\tau_{on}$ = 31 ± 7 sec. In similar experiments, at 20-msec voltage-step duration (▲), $\tau_{on}$ = 53 ± 2.5 sec.

TABLE 1

**Biophysical properties of *m*Kv1.3 wild-type, H404T mutant, and G380H mutant $K^+$ currents in RBL cells injected with the *m*Kv1.3 wild-type, H404T, and G380H cRNA**

All values were obtained from at least seven independent experiments and are given as mean ± standard deviation. Values for the cumulative inactivation were obtained by determining the peak current after the end of 10 pulses (200 msec) from −80 to +40 mV at 1 Hz.

| | *m*Kv1.3 wild-type | H404T mutant | G380H mutant |
|---|---|---|---|
| Activation | | | |
| $V_{½}$ (mV) | −28 ± 3 | −24 ± 5 | −25 ± 6 |
| $K$ | 6 ± 1 | 7 ± 2 | 6 ± 1 |
| $\tau_m$ (msec) | 4 ± 1 | 4 ± 2 | 4 ± 2 |
| Deactivation | | | |
| $\tau_t$ at −60 mV (msec) | 35 ± 7 | 44 ± 9 | 39 ± 8 |
| Inactivation | | | |
| $\tau_h$ at 40 mV (msec) | 227 ± 45 | ~1000 | >1000 |
| Cumulative inactivation current left (%) | 26 ± 5 | 98 ± 2 | 98 ± 2 |

during repeated pulses, as suggested by Jacobs and DeCoursey (24). To quantify this accumulation of block, we plotted the peak current amplitude before and during application of verapamil as a function of the time during the experiment, as shown for 20 μM verapamil in Fig. 1B. The reduction in peak current amplitude is almost independent of the duration of the pulse [compare 200-msec pulse duration (■) with 20-msec pulse duration (▲)] as long as the interpulse interval is constant (30 sec). This indicates that the reduction in the peak current amplitude in the presence of verapamil is due to an accumulation of block during the interpulse interval and not an effect of verapamil to accelerate C-type inactivation. This observation is in agreement with the results of Jacobs and DeCoursey (24), who concluded from the single-exponential time course of current decay in the presence of all concentrations of verapamil that the time course of current decay during application of verapamil reflects the rate at which open $K^+$ channels are being blocked.

To further quantify the accumulation of verapamil block on current through *m*Kv1.3, we investigated the effect of different concentrations of externally applied verapamil in the whole-cell configuration. In Fig. 2A (*top trace*), the application of verapamil leads to a dose-dependent block of the steady state peak $K^+$ currents (*bottom traces*) determined as in Fig. 1. The steady state peak current is reduced to 42% at a verapamil concentration of 10 μM. Normalized steady state peak currents are plotted against the applied verapamil concentrations in Fig. 2B (*smooth line*, expected dose-response curve if one verapamil molecule binds reversibly to one channel). This curve yields a dissociation constant $K_d$ value of 8 μM for the accumulated block of the *m*Kv1.3 current with externally applied verapamil. This value is in agreement with $K_d$ values from other examinations on Kv1.3 channels expressed either exogenously in *Xenopus laevis* oocytes or mammalian cells (10, 25) or endogenously in mouse and human T lymphocytes (25, 26).

To obtain further insight into the location of the binding site for verapamil, mutations were introduced into the *m*Kv1.3 $K^+$ channel. A schematic model of the putative pore region with flanking regions is shown to illustrate the position of the mutations (Fig. 3; the introduced mutations H404T and G380H are highlighted). The properties of these mutations in respect to the verapamil block should further elucidate the verapamil-interactive site on the channel.

The H404T current without verapamil shows slower C-type inactivation compared with the current through the wild-type channel (Fig. 4A, *top trace*, and Table 1). Also, the mutant G380H current shows slower C-type inactivation (see Table 1) and is as slow as that for H404T (data not shown). The changes in inactivation and other properties for these mutations have been described previously (16, 27). Verapamil accelerated the current decay of the H404T mutant channel with no significant accumulation of block during the interpulse interval (Fig. 4A). This was also true when the pulse duration was reduced from 200 to 20 msec (Fig. 4B) (i.e., the second trace after application of verapamil reached steady state peak current). In addition, block of the mutant H404T channel was dose dependent, and like the wild-type *m*Kv1.3 channel, the current decay was accelerated with higher concentrations of verapamil. In contrast to the wild-type current, the concentration of verapamil that produced a peak current reduction to 50% of the control current was 100–330 μM (Fig. 5A). In Fig. 5B, the normalized peak currents are plotted against the applied verapamil concentration. A fit to the data (Fig. 5B, *smooth line*) indicates that one verapamil molecule binds reversibly to one mutant channel, as seen for the *m*Kv1.3 wild-type channel, with a dissociation constant $K_d$ value for verapamil to block the steady state peak current of the mutant H404T channel of 195 μM. This was ~25-fold higher than the $K_d$ value for verapamil for the accumulated block of the *m*Kv1.3 wild-type channel. The

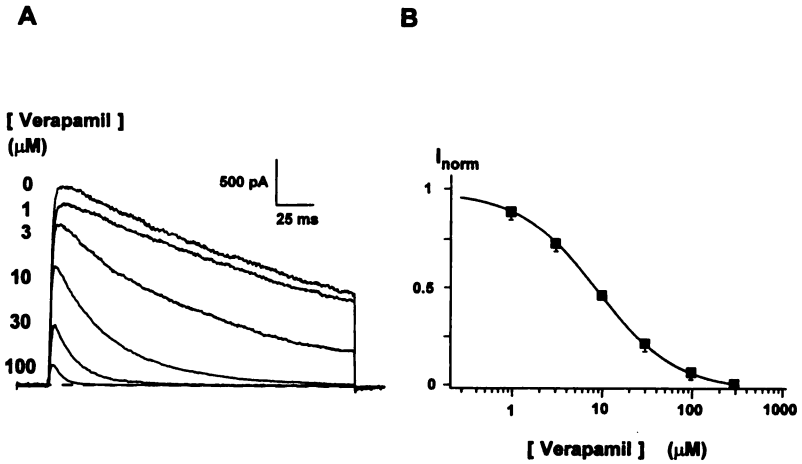


**Fig. 2.** Effect of extracellularly applied verapamil on steady state peak current through wild-type *m*Kv1.3 channels. A, Currents were elicited by 200-msec depolarizing voltage steps from a holding potential of −80 to +40 mV every 30 sec in the absence and presence of increasing concentrations of verapamil. Shown are steady state peak currents in the different solutions. The applied concentrations (in μM) are shown at each current trace. B, Dose-response curve for verapamil to block steady state peak current through *m*Kv1.3 channels. *Data points*, normalized current ($I_{norm} = I_{verapamil}/I_{control}$) from at least three independent experiments obtained by the indicated drug concentration. Mean ± standard deviation is indicated when it exceeds the size of the symbol. *Smooth line* was fitted to the measured data points ($I_{norm} = 1/\{1 + ([toxin]/K_d)\}$) and indicates a $K_d$ value for verapamil of 8 μM.

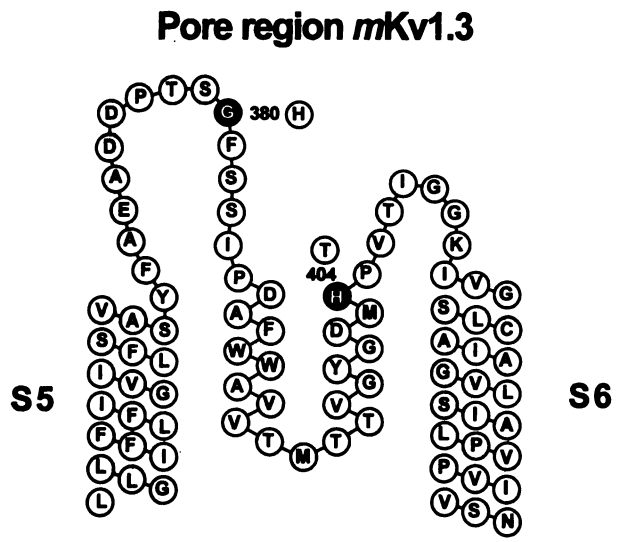


**Fig. 3.** Schematic model of the $K^+$ channel *m*Kv1.3 pore region of the $\alpha$ subunit. The amino acid sequence of the S5 segment, the putative pore segment, and the S6 segment are displayed. *Highlights*, positions of the two mutated amino acids G380 and H404. The derived mutations G380H and H404T are indicated.

dissociation constant $K_d$ value obtained for the G380H mutant was 208 $\mu$M (data not shown). This shows that the exchange of the external amino acids at positions 404 and 380 led to an alteration of the verapamil effect, although the affinity of verapamil to block the open channels seemed to be barely affected by the H404T mutation, as can be judged by a comparison of the current decay time constants in the presence of different verapamil concentrations.

This comparison is shown in Fig. 6. It can be seen that the current decay time constant $\tau_{decay}$ of current through the wild-type channel seemed to be 3–4-fold faster in the presence of similar verapamil concentrations compared with $\tau_{decay}$ of current through the H404T mutant channel. This apparent difference, however, might reflect the differences in intrinsic inactivation of the two channels (see Table 1), indicating that the open-channel block by verapamil in both channels was similar. The accumulation of block during the interpulse interval, however, can occur in the wild-type but not the mutant channel, suggesting that changes of amino acids in the outer vestibule have an effect on verapamil action.

To confirm this hypothesis of an external binding site and to exclude an internal binding site, we examined the effect of internally applied verapamil on the *m*Kv1.3 wild-type channel. Verapamil was applied to the internal side of the cell via the pipette solution in the whole-cell configuration (Fig. 7A). It is obvious that there is neither a peak current reduction nor a significant faster current decay when verapamil is applied internally at a concentration of $\leq$1 mM. The first pulse (Fig. 7A) recorded after whole-cell configuration was reached shows the normal *m*Kv1.3 current, and the second pulse, which was recorded 10 min later, shows no significant change in current properties. Verapamil applied internally through the pipette in the whole-cell configuration apparently cannot block the wild-type current. This result is in agreement with the results of DeCoursey (17). This apparent lack of internally applied verapamil on current through *m*Kv1.3 seemed to confirm our hypothesis of an external binding site of verapamil. Experiments with bath application of verapamil in inside-out patches, however, disproved this hypothesis (Fig. 7B). Wild-type current without verapamil (Fig. 7B, *top trace*) in an inside-out patch had properties that were quite similar to those of the current in the whole-cell configuration. The addition of 10 $\mu$M verapamil to the bath solution was sufficient to block approximately half of the *m*Kv1.3 wild-type steady state current (Fig. 7B, *bottom trace*). The time course of the development of this block was similar to that shown in Fig. 1 (data not shown). With 10 $\mu$M verapamil applied to the bath, there not only was a peak current reduction but also a faster current decay. This effect is comparable to the current decay acceleration caused by extracellular application of verapamil in the whole-cell configuration. The experiment indicates that verapamil is able to reach a binding site when applied to the bath in an inside-out patch. This last result is in contrast to the results obtained in investigations with the application of verapamil through the patch pipette in whole-cell configuration in which no effect could be seen on the *m*Kv1.3 current.

To elucidate these conflicting results, *N*-methyl-verapamil, a verapamil derivative, was used to determine whether verapamil acts from the inside or the outside on the *m*Kv1.3 wild-type channel. Due to an additional methyl group at the central nitrogen, this derivative lost the ability to become protonated and was permanently charged. For *N*-methyl-verapamil, it is nearly impossible to pass biological membranes (28). If this verapamil derivative acts on the same site as verapamil, it should be possible to distinguish the blocking effects that verapamil could cause if it passes the membrane to reach its binding site. In a first step, the affinity of *N*-methyl-verapamil on the *m*Kv1.3 wild-type channel had to be determined. Extracellularly applied *N*-methyl-verapamil on *m*Kv1.3 channels in the whole-cell configuration was able to block half of the wild-type currents with a $K_d$ value of ~1 mM (Fig. 8A). The current decay of the blocked current was only a little faster than that without drug. *N*-Methyl-verapamil applied extracellularly is a very weak blocker and >100-fold less potent as verapamil applied externally. These data are in agreement with the results of DeCoursey (17) and could be explained in one of two ways. First, this verapamil derivative has a lower affinity to the binding site due to its structural changes, or, second, it could not reach an internal binding site due to the membrane impermeability of *N*-methyl-verapamil. To distinguish between these two possibilities, we applied *N*-methyl-verapamil either through the patch pipette in the whole-cell mode (25 $\mu$M, Fig. 8B) or by changing the bath solution in an inside-out patch (10 $\mu$M, Fig. 8C). The two experiments gave similar results. The *m*Kv1.3 current showed a significant current reduction and a faster current decay in the presence of *N*-methyl-verapamil on the intracellular site. The two effects (blocking and acceleration of the current decay) were comparable to the effect of verapamil applied extracellularly (whole-cell) and intracellularly (inside-out patch) (Figs. 1A and 7B, respectively). *N*-Methyl-verapamil applied to the intracellular side of the membrane seemed to be as potent as verapamil. These results indicate the existence of (a) an external and an internal binding site for verapamil in which *N*-methyl-verapamil is able to bind to only the internal site or (b) just one internal binding site for verapamil and *N*-methyl-verapamil with nearly the same affinity for both compounds.

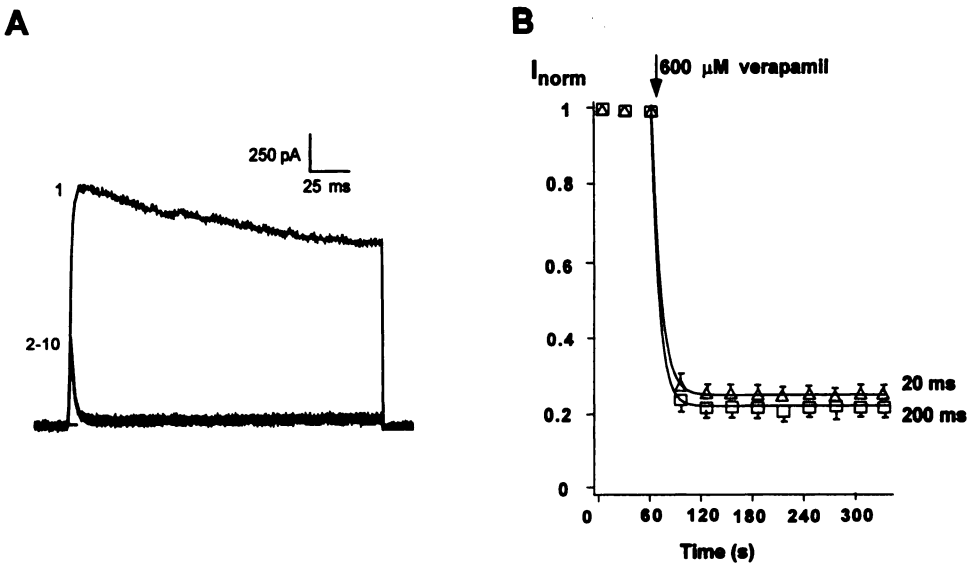


**Fig. 4.** Effect of extracellularly applied verapamil on currents through H404T mutant channels. A, Currents were elicited by 200-msec depolarizing voltage steps from a holding potential of −80 to +40 mV every 30 sec. Currents were recorded (*trace 1*) before and (*traces 2–10*) after external application of 600 μM verapamil. *Traces 3–10*, constant current properties with a steady state peak current. B, Time course of peak current reduction by verapamil. Normalized peak currents obtained from the record shown in A and similar records were plotted against time. *Arrow*, bath solution was exchanged to a bath solution containing 600 μM verapamil. Time constants of peak current reduction ($\tau_{on}$) were obtained by fitting with a single-exponential function (*smooth line*) to the data. *Data points*, normalized peak current of at least three independent experiments; *bars*, mean ± standard deviation. At a 200-msec voltage-step duration (□), $\tau_{on}$ = 7.2 ± 0.5 sec. In similar experiments, at a the 20-msec voltage-step duration (Δ), $\tau_{on}$ = 8.1 ± 1.1 sec.

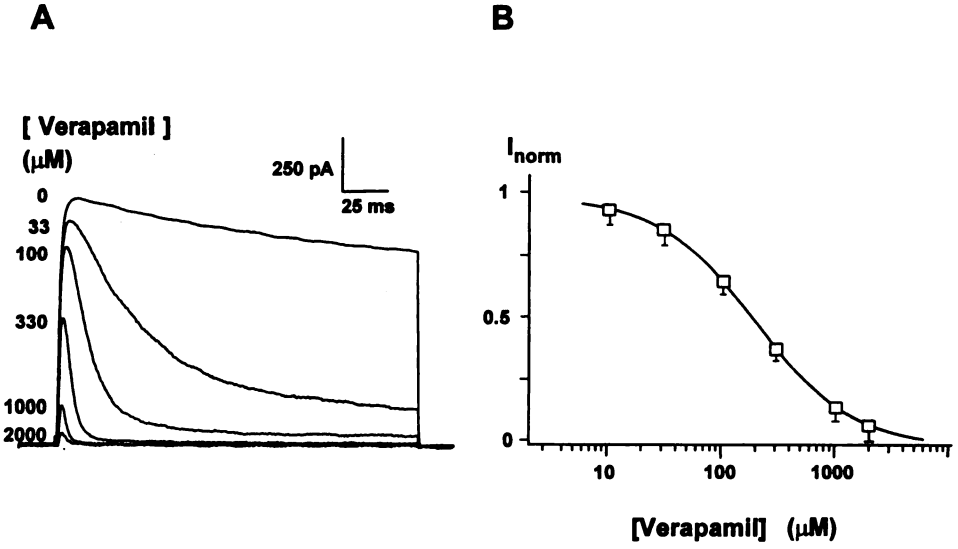


**Fig. 5.** Effect of extracellularly applied verapamil on steady state peak current through mutant *m*Kv1.3 H404T channels. A, Currents were elicited by 200-msec depolarizing voltage steps from a holding potential of −80 to +40 mV every 30 sec in the absence and presence of increasing concentrations of verapamil. Shown are steady state peak currents in the different solutions. The applied concentrations (in μM) are shown at each current trace. B, Dose-response curve for verapamil to block steady state peak current through mutant H404T channels. *Data points*, normalized current ($I_{norm}$ = $I_{verapamil}/I_{control}$) from at least three independent experiments obtained by the indicated drug concentration. Mean ± standard deviation is indicated when it exceeds the size of the symbol. The *smooth line* was fitted to the measured data points ($I_{norm}$ = 1/{1 + ([toxin]/$K_d$)} and indicates a $K_d$ value for verapamil of 195 μM.

A comparison of these results on the wild-type currents with the effect of verapamil and *N*-methyl-verapamil on mutant H404T currents could help to elucidate the location of the binding site. The effects of verapamil and *N*-methyl-verapamil on the mutant channel H404T were examined (Fig. 9). First, verapamil was applied to the bath solution on an inside-out patch (Fig. 9A). Verapamil (100 μM) in the bath solution led to a peak current reduction of approximately one third with a similar time course of peak current reduction, as shown in Fig. 4 for verapamil applied extracellularly in the whole-cell configuration on H404T currents (data not shown). The mutant H404T current decay was much faster in the presence of the drug and was similar to the current decay seen for externally applied verapamil to the mutant H404T current in the whole-cell configuration (Fig. 5A). From several experiments, we obtained a dissociation constant $K_d$ value of ~185 μM for verapamil to block steady state current through mutant H404T channel when applied in the bath solution on an inside-out patch. This was nearly the same concentration as obtained for externally applied verapamil in the dose-response experiments (Fig. 5). Verapamil blocked the mutant H404T current on an inside-out patch with similar $K_d$ and current decay values as verapamil applied extracellularly in the whole-cell configuration. The effect of *N*-methyl-verapamil on the H404T current and a comparison with the effect on wild-type currents should yield more information regarding the binding site of these compounds. The membrane-impermeable *N*-methyl-verapamil was applied extracellularly in the whole-cell configuration (Fig. 9B). The current (Fig. 9B, *top trace*) without drug showed the typical

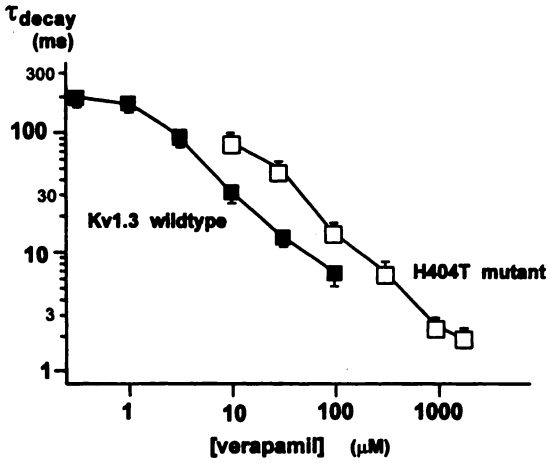


**Fig. 6.** Comparison of the current decay time constants ($\tau_{decay}$) of the (■) *m*Kv1.3 wild-type and (□) H404T mutant channel with different verapamil concentrations. $\tau_{decay}$ was obtained by fitting the current decay with a single-exponential function to the data. *Data points*, $\tau_{decay}$ at different concentrations of verapamil from at least five independent experiments; plotted against the externally applied concentration of verapamil. *Bars*, mean ± standard deviation.

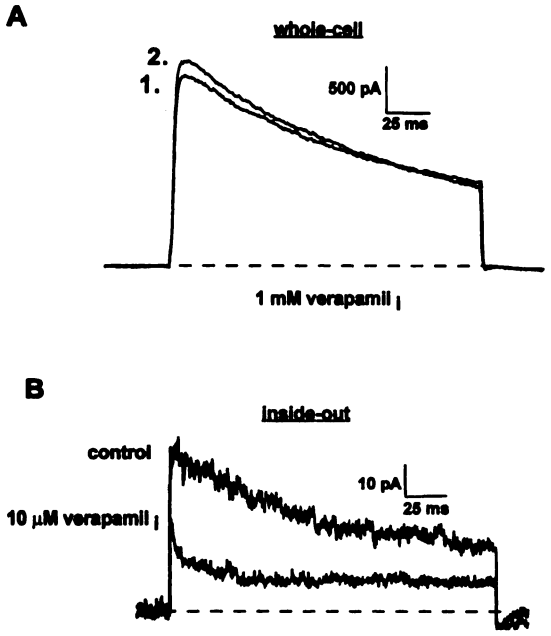


**Fig. 7.** Effect of intracellularly applied phenylalkylamines on steady state peak current through wild-type *m*Kv1.3 channels. Currents were elicited by 200-msec depolarizing voltage steps from a holding potential of −80 to +40 mV every 30 sec. A, Internal application of verapamil in the whole-cell configuration with 1 mM verapamil in the pipette solution. The first current trace was measured immediately after whole-cell configuration was reached. The second current trace was measured 10 min after the first trace. B, Application of 10 μM verapamil to the bath solution in an inside-out patch. *Bottom trace*, recorded 120 sec after verapamil application to the bath solution (steady state block). Block was reversible after wash-out.

slow inactivating mutant H404T current properties (Fig. 4A, top trace), and 1 mM *N*-methyl-verapamil blocked the steady state peak current only very weakly, with a little accelerated current decay (*bottom trace*). The dissociation constant $K_d$ value for *N*-methyl-verapamil to block steady state current was ~9 mM, and therefore *N*-methyl-verapamil was ~50-fold less potent than extracellularly applied verapamil. To test

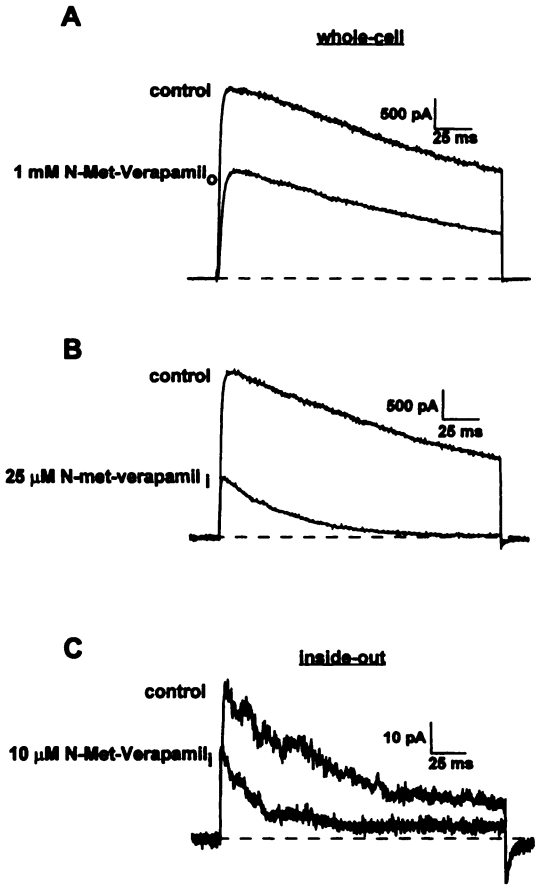


**Fig. 8.** Effect of *N*-methyl-verapamil on steady state peak current through wild-type *m*Kv1.3 channels. Currents were elicited by 200-msec depolarizing voltage steps from a holding potential of −80 to +40 mV every 30 sec. A, External application of 1 mM *N*-methyl-verapamil to the bath solution in the whole-cell configuration. *Bottom trace*, steady state current block 4 min after drug application. B, Internal application of *N*-methyl-verapamil in the whole-cell configuration with 25 μM *N*-methyl-verapamil in the pipette solution. *Top trace*, measured after whole-cell configuration was reached. *Bottom trace*, measured 5 min after top trace. C, Application of 10 μM *N*-methyl-verapamil to the bath solution in an inside-out patch. *Bottom trace*, recorded 120 sec after verapamil application to the bath solution (steady state block). Block was reversible after wash-out.

the potency of *N*-methyl-verapamil intracellularly, 200 μM *N*-methyl-verapamil was applied to the bath solution in an inside-out patch (Fig. 9C). The applied concentration blocked ~60% of the mutant steady state peak current and accelerated the current decay. These are the same effects as extracellularly and intracellularly applied verapamil on the mutant H404T currents (Figs. 5A and 9A). Taken together, verapamil blocked the mutant H404T current applied extracellularly and intracellularly on an inside-out patch with the same affinity, whereas the membrane-impermeable *N*-methyl-verapamil blocked the mutant H404T current only on an inside-out patch but with nearly the same $K_d$ value as verapamil.

A comparison of the results with verapamil and *N*-methyl-verapamil on the *m*Kv1.3 wild-type channel and the mutant H404T channel strongly supports the hypothesis that there is only one internal verapamil-binding site, which shows the same affinity for verapamil and *N*-methyl-verapamil and the same increased $K_d$ value for verapamil and *N*-methyl-verapamil in the H404T mutant as in the wild-type.

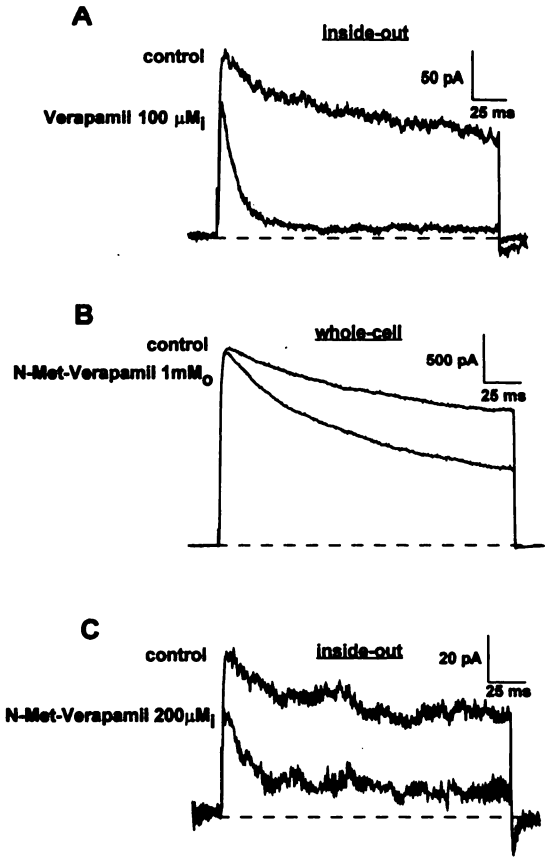


**Fig. 9.** Effect of verapamil and *N*-methyl-verapamil on steady state peak current through the mutant channel H404T. Currents were elicited by 200-msec depolarizing voltage steps from a holding potential of −80 to +40 mV every 30 sec. A, Application of 100 μM verapamil to the bath solution in an inside-out patch. *Bottom trace*, after steady state block was reached (60 sec after drug application to the bath). B, External application of 1 mM *N*-methyl-verapamil in the whole-cell configuration. The steady state block was reached 4 min after drug application. C, Application of 200 μM *N*-methyl-verapamil to the bath solution in an inside-out patch. *Bottom trace*, steady state blocked current (reached 60 sec after drug application). All blocks were reversible after wash-out.

If this hypothesis of an internal binding site is correct, drugs or compounds that are known to block *m*Kv1.3 from the outside (e.g., $TEA_o$ or $KTX_o$) would not be expected to compete with verapamil at their external binding site, whereas drugs that are known to block *m*Kv1.3 from the inside (e.g., $TEA_i$) would be expected to compete with verapamil if these compounds share the same internal binding site. In the first case, the efficacy of verapamil block should be independent of the presence of $TEA_o$ or $KTX_o$, whereas a competition for the same site should reduce the efficacy of verapamil block in the presence of $TEA_i$. In our competition experiments, we used 25 μM verapamil, which should reduce the steady state peak current by ~70% if no competition occurs (Fig. 2). In Fig. 10A, 16 mM $TEA_o$ was applied extracellularly in the whole-cell configuration to the *m*Kv1.3 wild-type channel. The current was significantly reduced (to 42%) and shows the typical slowed current decay (Fig. 10A, *middle trace*) (29). The addition of 25 μM verapamil to the 16 mM $TEA_o$ containing extracellularly applied solution led to an additional steady state current reduction of ~70% of the $TEA_o$ reduced current (Fig. 10A, *bottom trace*). This steady state current reduction is to be expected if the drugs act on different binding sites (see above). A similar experiment with $KTX_o$ and verapamil is shown in Fig. 10B. Extracellularly applied $KTX_o$ (1 nM) reduced the control current to ~45% (Fig. 10B, *middle trace*). The addition of 25 μM verapamil to the 1 nM $KTX_o$-containing extracellular solution led to a steady state current reduction of ~73% of the $KTX_o$ reduced current (Fig. 10B, *bottom trace*). This steady state current reduction caused by verapamil is also independent of the presence of $KTX_o$ (Fig. 1A). There was no competition of verapamil, with either $TEA_o$ or $KTX_o$, at the external binding site of these compounds. To examine the postulated internal binding site of verapamil, 200 μM $TEA_i$ was applied intracellularly via the pipette solution in the whole-cell configuration. The *m*Kv1.3 wild-type current reduced by the applied $TEA_i$ concentration is shown in Fig. 10C (*top trace*). Extracellular application of 25 μM verapamil with 200 μM $TEA_i$ led to a steady state current reduction of ~37% of the $TEA_i$ reduced current (Fig. 10C, *bottom trace*). This steady state current reduction is much weaker, which would be expected if verapamil acts independent of the presence of $TEA_i$, indicating that internal $TEA_i$ might compete for the same binding site with extracellularly applied verapamil. These results

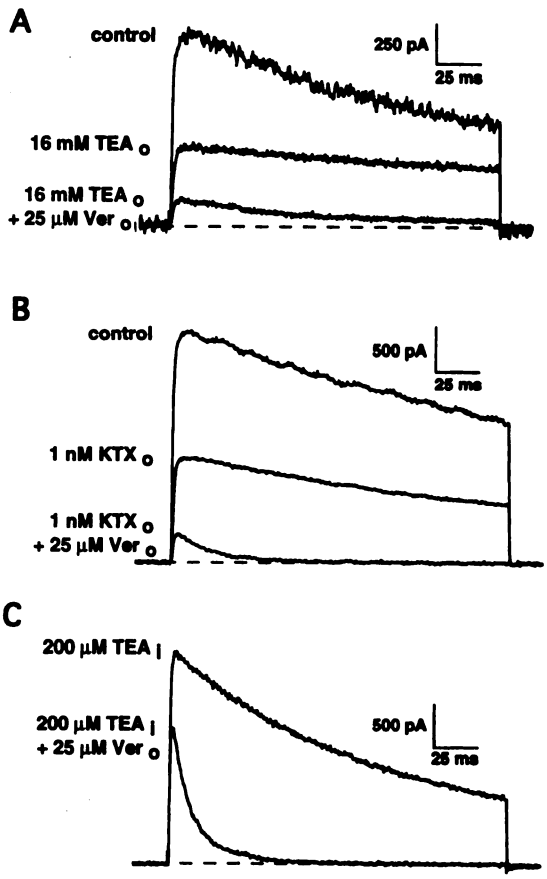


**Fig. 10.** Interaction of verapamil with KTX and TEA on the wild-type *m*Kv1.3 $K^+$ channel. Currents were elicited by 200-msec depolarizing voltage steps from a holding potential of −80 to +40 mV every 30 sec. A, Effect of 16 mM externally applied TEA alone (*middle*) and in combination with 25 μM externally applied verapamil. B, Effect of 1 nM externally applied KTX alone (*middle*) and in combination with 25 μM externally applied verapamil. C, Effect of 200 μM intracellularly applied TEA alone (*top*) and in combination with 25 μM externally applied verapamil (*bottom*). All experiments were done in the whole-cell configuration. Internal TEA was applied through the patch pipette.

provide further evidence that verapamil is passing through the membrane to reach its internal binding site on the *m*Kv1.3 wild-type channel.

## Discussion

To localize the site on the voltage-gated $K^+$ channel *m*Kv1.3 that is responsible for the investigated accumulation of the phenylalkylamine block, we investigated the effect of extracellularly and intracellularly applied verapamil and its quaternary derivative *N*-methyl-verapamil on $K^+$ steady state peak currents in RBL cells exogenously expressing the *m*Kv1.3 channel.

**Comparison with other channels.** Electrophysiological studies on L-type $Ca^{2+}$ and *n*-type $K^+$ channels showed that externally applied verapamil is able to block these channels, but different investigations with D575 and other quaternary phenylalkylamines have yielded different opinions regarding the *N*-methyl-verapamil effect on these channel types. For L-type $Ca^{2+}$ channels, it has been shown that phenylalkylamines bind to amino acid residues in S6 of the fourth domain of the $\alpha$ subunit (30; for a review, see Ref. 31). The binding site for phenylalkylamines seems to be localized at the internal site of the channel (32, 33), but recent investigations favor an external binding site for verapamil (34). On *n*-type $K^+$ channels in rat alveolar epithelial cells, DeCoursey (17) showed that extracellularly applied verapamil must partition into the membrane to reach its binding site and block the current. He could not see a comparable blocking effect of intracellularly applied verapamil and quaternary gallopamil (D890) on $K^+$ currents in these cells. Based on these findings, we performed experiments with phenylalkylamines showing that extracellularly applied verapamil is a potent blocker of *m*Kv1.3 steady state peak currents (Fig. 1), whereas the blocking potency of *N*-methyl-verapamil applied extracellularly was ~100-fold weaker than verapamil (Fig. 8A). These findings are comparable to results obtained by DeCoursey (17) on *n*-type $K^+$ channels and to results of investigations on L-type $Ca^{2+}$ channels (32).

**Effect of mutations on the outer vestibule.** The introduction of a mutation at the amino acid H404 and at the amino acid G380, located at the outer portion of the vestibule of the *m*Kv1.3 wild-type channel (Fig. 3), resulted in a much lower potency to accumulate block with extracellularly applied verapamil on the mutant steady state peak current compared with the wild-type (Fig. 5). The open-channel block was quite similar between the wild-type and the H404T mutant (Fig. 6). Determination of the steady state peak current reduction by verapamil yielded a $K_d$ value that was 25-fold higher for the mutant (Fig. 5). This reflects qualitatively the influence of the accumulation on the steady state peak current reduction caused by the wild-type. The externally located amino acid residue H404T mutant affected the blocking properties of the investigated phenylalkylamines through a loss of the ability to accumulate block of peak currents. The effect of extracellularly applied *N*-methyl-verapamil on the mutant H404T current was shifted to lower potencies in a comparable manner (Fig. 9B). These findings initially suggested that an extracellular binding site for verapamil was responsible for block accumulation due to the alteration of the accumulation affinity when responsible residues on the outside were exchanged, as shown for the H404T and G380H mutants. Other possible interpretations of the mutation effects are discussed below.

**Intracellular application of phenylalkylamines.** When we applied verapamil intracellularly via the pipette (≤1 mM), the compound was ineffective in blocking the *m*Kv1.3 current; this seemed to be further evidence for an external binding site and was comparable to observations with intracellularly applied phenylalkylamines via the pipette made by DeCoursey (17) on *n*-type $K^+$ channels and by Wegener and Nawrath (34) on L-type $Ca^{2+}$ channels. However, these findings were in contrast to previous studies on L-type $Ca^{2+}$ channels, in which verapamil or other tertiary phenylalkylamines applied intracellularly via the patch pipette were potent current blockers. Because of these contrary results with $Ca^{2+}$ channels and due to the possibility that tertiary phenylalkylamines can diffuse easily through biological membranes, whereas quaternary phenylalkylamines are not able to cross membranes, we performed experiments using inside-out patches to elucidate the possibility that the obtained results were dependent on the membrane permeability of the investigated phenylalkylamines. Surprisingly, using inside-out patches, we found the same blocking efficacy of internally applied verapamil on *m*Kv1.3 steady state peak currents compared with externally applied verapamil (Fig. 4B). This is in contrast to our (current report) and other (17, 34) investigations with intracellularly applied verapamil via the pipette in which no blocking effect was obtained. One possible explanation for this discrepancy is that pipette-applied verapamil may diffuse more rapidly through the membrane into the bath solution than it can accumulate to effective concentrations in the cell on the internal binding site of the channel. This hypothesis was described in detail by DeCoursey (17) and would account for the ineffectiveness of verapamil applied through the pipette. Another, perhaps additional, possibility is that verapamil has the ability to diffuse through intracellular membranes into organelles and other cellular structures or to bind unspecifically to membranes of these compartments, thereby diminishing the effective intracellular concentration of applied drug.

Additional evidence for these two possibilities comes from experiments in which *N*-methyl-verapamil was applied either via the pipette in the whole-cell configuration (Fig. 8B) or through bath application in an inside-out patch (Fig. 8C), showing nearly the same effects on reducing wild-type steady state peak currents as verapamil applied extracellularly in whole-cell (Fig. 1) or intracellularly on inside-out patches (Fig. 7B). A simple explanation for this effect of *N*-methyl-verapamil applied via the pipette is its membrane impermeability, so it is not possible for this compound to diffuse through or bind to membranes, a mechanism postulated for verapamil. *N*-Methyl-verapamil can accumulate to active concentrations in the cell when applied through the patch pipette and reaches its internal binding site.

It is therefore possible that in some cell types, tertiary phenylalkylamines applied through the patch pipette could have no or little effect compared with externally applied phenylalkylamines. This was the case for RBL cells exogenously expressing *m*Kv1.3 (current report), for rat alveolar epithelial cells endogenously expressing Kv1.3 (17), and for rat ventricular myocytes endogenously expressing L-type $Ca^{2+}$ channels (34). In other cell types, possibly lacking those intracellular organelles, there might not be a difference for

phenylalkylamines applied via the patch pipette compared with external application, as was the case for cat heart ventricular trabeculae (32) and guinea pig ventricular heart cells (33), endogenously expressing L-type $Ca^{2+}$ channels. Therefore, tertiary phenylalkylamines applied through the pipette could show the above behavior and would have no or less effect compared with externally applied phenylalkylamines, as shown by DeCoursey (17) and Wegener and Nawrath (34) and in the current report, or they can reach effective concentrations and are able to block ionic currents, as described by other investigators for L-type $Ca^{2+}$ channels (32, 33).

**Verapamil and *N*-methyl-verapamil.** *N*-Methyl-verapamil applied intracellularly in an inside-out patch of the wild-type channel and the H404T mutant was able to block steady state peak currents with comparable potency to verapamil (Figs. 8C and 9C). It had previously been shown that intracellularly applied quaternary phenylalkylamines were able to block L-type $Ca^{2+}$ currents, even if they had no such effect when applied externally (32, 33). Due to the membrane impermeability of quaternary phenylalkylamines, they would have only very limited access to an putative internal binding site if applied externally; that would explain the low potency of extracellularly applied *N*-methyl-verapamil on the *m*Kv1.3 wild-type channel as well as on the H404T mutant. Due to the same blocking efficiency of verapamil and *N*-methyl-verapamil at the internal site of the *m*Kv1.3 channel, the low blocking efficiency of externally applied *N*-methyl-verapamil could be explained by a low intrinsic concentration and not by a lower affinity for an assumed external binding site caused by the structural changes of the quaternary derivative. A model can be postulated for drug access to an internal binding site, as follows. Externally applied verapamil (pK = ~8.5) must first become uncharged to pass the membrane and then reach the internal binding site, where it binds in its active form. This model is quite similar to models postulated for the internal action of externally applied local anesthetics on $Na^+$ channels (35) and the action of externally applied 4-aminopyridine on *n*-type $K^+$ channels (36).

**Competition experiments.** The above results strongly support the hypothesis of an internal binding site for verapamil and *N*-methyl-verapamil on the *m*Kv1.3 channel. Further evidence for this model comes from competition experiments that we performed with verapamil and well-defined external and internal *m*Kv1.3 channel blockers. We could show that externally applied KTX as well as externally applied $TEA_o$, both of which are compounds that are not able to pass biological membranes and that have been shown to interact with amino acids on the outer mouth of the $K^+$ channel vestibule (16, 18), do not compete with externally applied verapamil for the same binding site. The blocking and accumulation effect of verapamil was as potent as it was without the simultaneous application of these drugs (Fig. 10, A and B). In contrast, internally applied $TEA_i$ led to a much lower potency of steady state block accumulation with extracellularly applied verapamil, whereas the open-channel block was unaffected. The reduced accumulation potency would not have been expected if verapamil block accumulation of *m*Kv1.3 steady state peak currents is independent of the presence of $TEA_i$ (Fig. 10C). From these results, we conclude that externally applied verapamil passes through the membrane and competes with intracellularly applied $TEA_i$ for the same site or portions of the same site responsible for accumulation and therefore shows less potent accumulation effects than when applied alone. This observation is further evidence for the postulated internal binding site responsible for the accumulation of block of verapamil and *N*-methyl-verapamil.

**External mutations affecting an internal binding site?** The much lower blocking effect of verapamil on the H404T and G380H mutant steady state peak currents indicates a strong influence of these mutations, localized at the outer vestibule, on the verapamil binding site, which is responsible for accumulation of block. Both the experiments on inside-out patches with verapamil and *N*-methyl-verapamil and the competition experiments clearly indicate an internal binding site. How could we explain that mutations at the outer vestibule of the channel alter the block accumulation potency of phenylalkylamines on an internally localized binding site in such a way? One has to conclude that the mutations affect not only structures in the local environment of the external mutations but also channel structures farther from these mutations. Those structural changes could even extend to the internal site of the pore region. Another mechanism by which the channel might show structural changes is through a change in the C-type inactivation. However, evidence has accumulated that the time course of C-type inactivation occurs on structures localized externally on the outer mouth of the pore. For example, externally applied TEA competes with the C-type inactivation (27, 37), and externally elevated concentrations of $K^+$ and $Ca^{2+}$ alter C-type inactivation (25, 38). However, there also is evidence that the C-type inactivation occurs not only on structures of the external vestibule but also on structures deeper in the pore and in the S6 segment. It could be shown that mutations at positions T449 (equal to position H404 in *m*Kv1.3) and A463 (located in S6) in the *Shaker* channel, lacking *n*-type inactivation (39), and the mutation A413V (located in S6) in the Kv1.3 channel (40) affect the C-type inactivation. The P-type inactivation, perhaps another related inactivation process, could be produced by a mutation deep in the pore (41). Therefore, it can be imagined that larger portions of channel structures must undergo conformational changes during the C-type inactivation compared with only externally localized amino acid structures. The investigated mutations H404T and G380H show a slower C-type inactivation compared with the *m*Kv1.3 wild-type. However, a more pronounced effect of these two mutations can be observed during recovery from this type of inactivation, as can be seen by a change in the "use dependence" property of *m*Kv1.3 (Table 1). The change in this property might be connected to the inability of verapamil block to accumulate during the interpulse interval and must be envisioned as a conformational change occurring at the intracellular side of the channel. Therefore, it is possible that mutations that led to strong alterations of the recovery from C-type inactivation, like H404T and G380H in the *m*Kv1.3 channel, affect not only structures in the local external environment of the mutations, such as those described above, but also channel structures farther from these mutations. Such structures, perhaps portions of the C-type inactivation mechanism or portions of the mechanism responsible for recovery from inactivation, could extend even to the internal site of the pore region. Our data indicate the possibility that mutations on the outer vestibule

of the *m*Kv1.3 pore can alter an internal binding site of phenylalkylamines.

Taken together, we demonstrated that (a) verapamil and *N*-methyl-verapamil, a tertiary and a quaternary phenylalkylamine, bind to an internal binding site on the *m*Kv1.3 channel with high potency; (b) the blocking potency of these phenylalkylamines when applied externally depends on their membrane permeability and is very low for the quaternary *N*-methyl-verapamil (D575) and the charged verapamil; and (c) the internal binding site, which is responsible for accumulation of steady state peak current block, is probably affected by single-point mutations localized in the outer part of the *m*Kv1.3 pore region.

**Acknowledgments**

For the excellent technical support, we wish to thank Christine Hanselmann. We thank Dr. K. George Chandy (University of California, Irvine, Irvine, CA) for his generous gift of the *m*Kv1.3 mutants and Dr. G. Paul and Dr. M. Raschack (Knoll, Ludwigshafen, Germany) for the kind gift of D575.

**References**

1. DeCoursey, T. E., K. G. Chandy, S. Gupta, and M. D. Cahalan. Voltage-gated $K^+$ channels: a role in mitogenesis? *Nature (Lond.)* **307**:465–468 (1984).
2. Chandy, K. G., T. E. DeCoursey, M. D. Cahalan, C. McLaughlin, and S. Gupta. Voltage-gated potassium channels are required for human T-cell activation. *J. Exp. Med.* **160**:369–385 (1984).
3. Cahalan, M. D., K. G. Chandy, T. E. DeCoursey, and S. Gupta. A voltage-gated potassium channel in human T lymphocytes. *J. Physiol.* **358**:197–237 (1984).
4. Miller, C. Annus Mirabilis of potassium channels. *Science (Washington D. C.)* **252**:1092–1096 (1990).
5. Hartmann, H. A., G. E. Kirsch, J. A. Drewe, M. Taglialatela, R. H. Joho, and A. M. Brown. Exchange of conduction pathways between two related $K^+$ channels. *Science (Washington D. C.)* **251**:942–944 (1991).
6. Papazian, D. M., L. C. Timpe, Y. N. Jan, and L. Y. Jan. Alteration of voltage-dependence of *Shaker* potassium channel by mutations in the S4 sequence. *Nature (Lond.)* **349**:305–310 (1991).
7. Jan, L. Y., and Y. N. Jan. Structural elements involved in specific $K^+$ channel functions. *Annu. Rev. Physiol.* **54**:537–555 (1992).
8. Pongs, O. Molecular biology of voltage-dependent potassium channels. *Physiol. Rev.* **72**:69–88 (1992).
9. Pongs, O. *Shaker*-related $K^+$ channels. *Semin. Neurosci.* **5**:93–100 (1993).
10. Grissmer, S., B. Dethlefs, J. J. Wasmuth, A. L. Goldin, G. A. Gutman, M. D. Cahalan, and K. G. Chandy. Expression and chromosomal localization of a lymphocyte $K^+$ channel gene. *Proc. Natl. Acad. Sci. USA* **87**:9411–9415 (1990).
11. Cai, Y. C., B. Peregrine, R. A. North, D. C. Dooley, and J. Douglass. Characterization and functional expression of genomic DNA encoding the human lymphocyte type N potassium channel. *DNA Cell Biol.* **11**:163–172 (1992).
12. Price, M., S. C. Lee, and C. Deutsch. Charybdotoxin inhibits proliferation and interleukin 2 production in human peripheral blood lymphocytes. *Proc. Natl. Acad. Sci. USA* **89**:10171–10175 (1989).
13. Sands, S. B., R. S. Lewis, and M. D. Cahalan. Charybdotoxin blocks voltage gated $K^+$ channels in human and murine T lymphocytes. *J. Gen. Physiol.* **93**:1061–1074 (1989).
14. Romi, R., M. Crest, M. Gola, F. Sampieri, G. Jacquet, H. Yerrouk, P. Mansuelle, O. Sorokine, A. Van Dorsselaer, H. Rochat, M.-F. Martin-Eauclaire, and J. Van Rietschoten. Synthesis and characterization of kaliotoxin: is the 26–32 sequence essential for potassium channel recognition? *J. Biol. Chem.* **268**:26302–26309 (1993).
15. Garcia-Carvo, M., R. J. Leonard, J. Novick, S. P. Stevens, W. Schmalhofer, G. J. Kaczorowski, and M. L. Garcia. Purification, characterization, and biosynthesis of margatoxin, a component of *Centruroides margaritatus* venom that selectively inhibits voltage-dependent potassium channels. *J. Biol. Chem.* **268**:18866–18874 (1993).
16. Aiyar, J., J. M. Withka, J. P. Rizzi, D. H. Singleton, G. C. Andrews, W. Lin, J. Boyd, D. C. Hanson, M. Simon, B. Dethlefs, C. Lee, J. E. Hall, G. A. Gutman, and K. G. Chandy. Topology of the pore-region of a $K^+$ channel revealed by the NMR-derived structures of scorpion toxins. *Neuron* **15**:1169–1181 (1995).
17. DeCoursey, T. E. Mechanism of $K^+$ channel block by verapamil and related compounds in rat alveolar epithelial cells. *J. Gen. Physiol.* **106**:745–779 (1995).
18. MacKinnon, R., and G. Yellen. Mutations affecting TEA blockade and ion permeation in voltage-activated $K^+$ channels. *Science (Washington D. C.)* **250**:276–279 (1990).
19. Rauer, H. J., Hanselmann, C., and S. Grissmer. Pharmacological characterization of the voltage-gated potassium channel Kv1.3 and a G380H mutant (Abstract). *Biophys. J.* **70**:A400 (1996).
20. Rauer, H. J., and S. Grissmer. Block of $Ca^{2+}$ channel antagonists on wildtype and mutant Kv1.3 potassium channels. *Pflueg. Arch. Eur. J. Physiol.* **431**:R84 (1996).
21. Eccleston, E., B. J. Leonard, J. S. Lowe, and H. J. Welford. Basophilic leukaemia in the albino rat and a demonstration of the basopoietin. *Nature New Biol.* **244**:73–76 (1973).
22. Hamill, O. P., A. Marty, E. Neher, B. Sakmann, and F. J. Sigworth. Improved patch-clamp techniques for high-resolution current recording from cells and cell-free membrane patches. *Pflueg. Arch.* **391**:85–100 (1981).
23. Krieg, P. A., and D. A. Melton. Functional messenger RNAs are produced by SP6 *in vitro* transcription of cloned cDNAs. *Nucleic Acids Res.* **12**:7057–7070 (1984).
24. Jacobs, E. R., and T. E. DeCoursey. Mechanism of potassium channel block in rat alveolar epithelial cells. *J. Pharmacol. Exp. Ther.* **255**:459–472 (1990).
25. Chandy, K. G., S. Gutman, and S. Grissmer. Physiological role, molecular structure and evolutionary relationships of voltage-gated potassium channels in T lymphocytes. *Semin. Neurosci.* **5**:125–134 (1993).
26. DeCoursey, T. E., K. G. Chandy, S. Gupta, and M. D. Cahalan. Voltage dependent ion channels in T lymphocytes. *J. Neuroimmunol.* **10**:71–95 (1985).
27. Lopez-Barneo, J., T. Hoshi, S. H. Heinemann, and R. W. Aldrich. Effect of external cations and mutations in the pore region on C-type inactivation of *Shaker* potassium channels. *Recept. Channels* **1**:66–71 (1993).
28. Retzinger, G. S., L. Cohen, S. H. Lau, and F. J. Kezdy. Ionization and surface properties of verapamil and several verapamil analogues. *J. Pharm. Sci.* **75**:976–982 (1986).
29. Grissmer, S., and M. D. Cahalan. TEA prevents inactivation while blocking open $K^+$ channels in human T lymphocytes. *Biophys. J.* **55**:203–206 (1989).
30. Striessnig, J., H. Glossmann, and W. A. Catterall. Identification of a phenylalkylamine binding region within the $\alpha 1$ subunit of skeletal muscle $Ca^{2+}$ channels. *Proc. Natl. Acad. Sci. USA* **87**:9108–9112 (1990).
31. Spedding, M., and R. Paoletti. Classification of calcium channels and the site of action of drugs modifying channel function. *Pharmacol. Rev.* **44**:363–376 (1992).
32. Hescheler, J., D. Pelzer, G. Trube, and W. Trautwein. Does the organic calcium channel blocker D600 act from inside or outside on the cardiac cell membrane? *Pflueg. Arch. Eur. J. Physiol.* **393**:287–291 (1982).
33. Lee, K. S., and R. W. Tsien. High selectivity of calcium channels in single dialysed heart cells of the guinea-pig. *J. Physiol.* **354**:253–272 (1983).
34. Wegener, J. W., and H. Nawrath. Extracellular site of action of phenylalkylamines on L-type calcium current in rat ventricular myocytes. *Naunyn-Schmiedeberg's Arch. Pharmacol.* **352**:322–330 (1995).
35. Cahalan, M. D., B. I. Shapiro, and W. Almers. Relationship between inactivation of sodium channels and block by quaternary derivatives of local anesthetics and other compounds, in *Progress in Anesthesiology: 2. Molecular Mechanism of Anesthesia*. Raven Press, New York, 17–33 (1980).
36. Choquet, D., and H. Korn. Mechanism of 4-aminopyridine action on voltage-gated potassium channels in lymphocytes. *J. Gen. Physiol.* **99**:217–240 (1992).
37. Choi, K. L., R. W. Aldrich, and G. Yellen. Tetraethylammonium blockade distinguishes between two inactivation mechanisms in voltage-activated $K^+$ channels. *Proc. Natl. Acad. Sci. USA* **88**:5092–5095 (1991).
38. Grissmer, S., and M. D. Cahalan. Divalent ion trapping inside potassium channels of human T lymphocytes. *J. Gen. Physiol.* **93**:609–630 (1989).
39. Ogielska, E. M., W. N. Zagotta, T. Hoshi, S. H. Heinemann, J. Haab, and R. W. Aldrich. Cooperative subunit interaction in C-type inactivation of K channels. *Biophys. J.* **69**:2449–2457 (1995).
40. Panyi, G., Z. Sheng, L. Tu, and C. Deutsch. C-type inactivation of a voltage-gated $K^+$ channel occurs by a cooperative mechanism. *Biophys. J.* **69**:896–903 (1995).
41. De Biasi, M., Hartmann, H. A., Drewe, J. A., Taglialatela, M., Brown, A. M., and G. E. Kirsch. Inactivation determined by a single site in $K^+$ pores. *Pflueg. Arch. Eur. J. Physiol.* **422**:354–363 (1993).

**Send reprint requests to:** Dr. S. Grissmer, Department of Applied Physiology, University of Ulm, 89075 Ulm, Germany. E-mail: stephan.grissmer@medizin.uni-ulm.de .